Scientia Iranica (2024) 31(17), 1547–1555

SCIENTIA IRANICA

Sharif University of Technology

Scientia Iranica

Transactions D: Computer Science & Engineering and Electrical Engineering

https://scientiairanica.sharif.edu

Half hexagonal shaped UWB antenna with triple band notch using resonating structures for wireless communication

Ushaben Keshwala[a], Sanyog Rawat[b], and Kanad Ray[c,*]

a. *Department of Computer Science and Engineering, Amity University Uttar Pradesh, Noida, India.*
b. *Manipal University Jaipur, Jaipur-Ajmer Express Highway, Dehmi Kalan, Near GVK Toll Plaza, Jaipur, Rajasthan, India.*
c. *Amity University Rajasthan, SP-1, Kant Kalwar, NH-11C, RIICO Industrial Area, Jaipur, Rajasthan, India.*

Received 17 October 2021; received in revised form 11 July 2022; accepted 1 May 2023

KEYWORDS
Half hexagonal monopole;
Resonating structures;
Ultra-wide band antenna;
Band notch characteristics;
Defected ground structure.

Abstract. In this article, an UWB (Ultra-Wide Band) compact monopole antenna with triple band-notched characteristics is presented. The antenna structure consists of a half-hexagon monopole with rectangular and square resonant spirals structures for the exclusion of frequency bands for WiMAX (3.25–3.85 GHz), WLAN (5.15–5.85 GHz), and Fixed/Mobile Satellite Communication (7.55–7.75 GHz). The compact antenna of size 28×29 mm^2 achieves simulated ultra-wide bandwidth of 14.7 GHz (2.9 GHz–17.6 GHz) and measured bandwidth of 14.8 GHz (3.21–18.0 GHz). The stable gain characteristic is obtained for the passband and gain is reduced to −2.02 dBi (3.57 GHz), 0.4 dBi (5.3 GHz) and −2.75 dBi (7.6 GHz) at band notch frequencies.

1. Introduction

The UWB antennas have been attracting many researchers' attention after the declaration of the 3.1–10.6 GHz band for ultra-wideband applications by the FCC [1] for commercial use. Many advantages of the UWB include ultra-wide commercial bandwidth, high data rate, compact size, etc., though there are many advantages, the UWB system faces many implementation challenges like multipath fading and co-channel interferences due to the coexisting of communication systems i.e., WiMAX band, WLAN bands, and fixed satellite/mobile communication. By keeping these issues in mind it is desirable to have multi-band-notch characteristics in the antenna which is incorporated in UWB systems.

Various methods have been proposed to achieve band-notch characteristics [2–19]. The most common technique is to cut a slot on the patch or the feed line and the ground plane. In this, the position and size of the slot determine the middle frequency and the bandwidth of the notch. In slot techniques, a quarter-wavelength or half wavelength of different shapes such as U-shaped, L-shaped, split ring resonators are cut in the patch or the ground plane [2–12]. Although the slot methods are efficient in generating band notches, only single or double notches can be produced [3]. Various

*. *Corresponding author.*
E-mail address: kray@jpr.amity.edu (K. Ray)

To cite this article:
U. Keshwala, S. Rawat, and K. Ray "Half hexagonal shaped UWB antenna with triple band notch using resonating structures for wireless communication", *Scientia Iranica* (2024), **31**(17), pp. 1547-1555
https://doi.org/10.24200/sci.2023.59268.6145

antenna geometries have been proposed to acquire the single-band and dual-band rejection characteristics obtained using different shapes of slots on the patch [4,5], parasitic slits [6], inserting CSRR (Complementary Split-Ring Resonator) in the microstrip line feed [7], or by using EBG cells [8]. In [9] parasitic coupled loops/resonators are used for achieving multiple band-notches. In [10] semi-circular patch antenna incorporated with a complementary split ring for a dual-band notch is presented. The quasi self-complementary semi octagonal-shaped UWB antenna with a single-band notch (5.15–5.85 GHz) with a bandwidth of 2.9–20 GHz is proposed in [11]. In [12] a circular monopole antenna with mushroom-shaped EBG structure is presented for UWB applications with band-notched characteristics. An asymmetric U-shaped monopole antenna with a T-shaped strip of size 20×36 mm^2 has been proposed [13]. A novel hp-shaped hexa-band frequency reconfigurable antenna for multi-standard wireless communication has been proposed [14].

The antenna presented and analysed in this article is a simple half-hexagonal with triple-band notch characteristics. The antenna proposed is realized in two stages. In the first stage, a half-hexagon monopole is presented to achieve UWB characteristics. In the second stage, three self-resonating spiral resonators are added; two resonating spirals are coupled with the feed line and one in the ground.

2. Antenna structure design and analysis

2.1. Basic UWB monopole design

The proposed structure is designed on the FR-4 substrate with $\varepsilon_r = 4.3$, $\tan\delta = 0.025$. The antenna has a compact size of $28 \times 29 \times 1.59$ mm^3. The front view and rear view of the designed antenna for triple band-notched characteristics are shown in Figure 1(a) and (b) respectively. The enlarged view of self-resonating spiral structures is depicted in Figure 1(c).

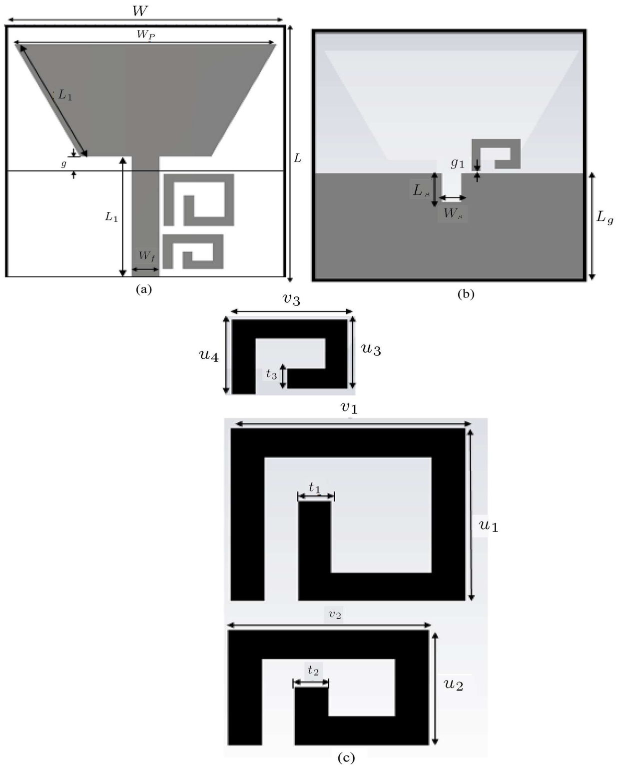

Figure 1. Half hexagonal antenna (a) Front view; (b) Back view and (c) Spiral structures.

The antenna feed is given by the microstrip line of width $W_f = 2.74$ mm. The optimized dimensions are presented in Table 1. The lower cut-off frequency corresponding to $VSWR = 2$ is calculated by using Eq. (1) [15], with all the dimensions are in cm.

$$f_L = \frac{7.2}{(l + r + g)}, \quad (1)$$

where 'l' and 'r' are respectively the length and radius of the corresponding cylindrical monopole antenna. For

Table 1. Optimised geometrical parameters of an antenna.

Antenna parameter	Values (mm)	Antenna parameter	Values (mm)	Antenna parameter	Values (mm)
L	29	u_2	4	v_1	7
W	28	u_3	3.5	u_1	6
L_g	12.5	u_4	3.8	g_1	0.3
L_f	14	L_1	13	v_2	6
W_f	2.8	L_s	2.5	v_3	5
$t_1 = t_2 = t_3$	1	Ws	2	g	1.5
L_{out1} (outer turn side length of spiral 1)	6	L_{out2} (outer turn side length of spiral 2)	4	L_{out3} (outer turn side length of spiral 3)	3.5
Sp_1 (total length of resonating spiral 1)	24.28	Sp_2 (total length of resonating spiral 2)	20	Sp_3 (total length of resonating spiral 3)	14.9

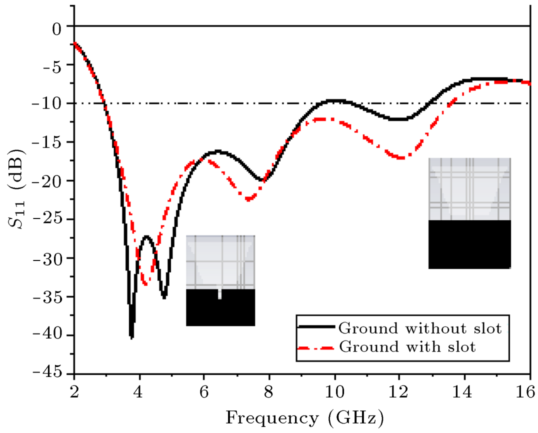

Figure 2. Simulated S_{11} (Return loss) plot for DGS and without DGS.

the hexagon of side length $L_1 = 1.3$ cm and ground-patch gap $g = 0.15$ cm, the value of cut-off frequency is 3.0 GHz. The l and r of the cylindrical monopole are related to the hexagonal monopole as follows [15],

$$l = \sqrt{3L_1}, \tag{2}$$

$$r = \frac{3L_1}{4}. \tag{3}$$

With the above geometrical parameters of an antenna and ground of size $L_g = 12.5$ mm the impedance bandwidth obtained (Reflection coefficient ($S11$) $<$ -10 dB) is $2.8 - 9.5$ GHz as it can be depicted in Figure 2, indicated with the partial ground without slot. The obtained impedance bandwidth does not cover the whole ultra-wideband of $3.1 - 10.6$ GHz; the next step is to increase the higher cut-off frequency of an antenna to cover the full UWB band by introducing a slot in the ground. Thus the partial ground is altered to DGS (Defected Ground Structure) with a rectangular slot on the upper side of the ground as shown in Figure 1(b). The length and the width of the rectangular slot are $L_s = 2.5$ mm and $W_s = 2$ mm, which gives a 5 mm slot. The length of the ground slot is calculated as [15]:

$$L_{gslot} = \frac{\lambda_g}{4} = \frac{\lambda}{4\sqrt{\varepsilon_{reff}}} = \frac{c}{4f_{10.6GHz}\sqrt{\varepsilon_{reff}}}. \tag{4}$$

As a consequence of the ground slot, the impedance bandwidth is expanded from $3 - 9.5$ GHz to $2.9 - 13.56$ GHz and the high cut off frequency is shifted to 13.56 GHz from 9.5 GHz as shown in Figure 2. After the acquisition of the UWB range, the next step in the design is to introduce band notches to suppress the existing interferences.

3. Basic design of resonating spirals for band notch

To achieve band notch characteristics self-resonating spiral structures are introduced. The dimensions of the spiral structures are calculated and optimized according to techniques given in [9]:

$$L_{Total} = \frac{4NL_{out} - [2N(1+N) - 3](S+t_1)}{\mathrm{N}}, \tag{5}$$

$$\mathrm{N_{normalized}} = \text{integer part of} = \frac{\mathrm{L_{out}} - (\mathrm{S} + \mathrm{t_1})}{2(\mathrm{S} + \mathrm{t_1})}. \tag{6}$$

In this N is the number of turns, $L_{out} = u_1$ is the outer turn side length, S the gap between turns; t_1 is the spiral width and the total effective length of spiral i.e.:

$$L_{Total} \approx L_1 \approx L_{eff} \approx \frac{C}{2f_{c\sqrt{\varepsilon_{\mathrm{reff}}}}}. \tag{7}$$

Which is nothing but half of the guided wavelength. Here in this C is the speed of light in free space; ε_{reff} is the effective dielectric constant. To calculate L_{total} for WiMAX (3.25–3.85 GHz) the f_c is taken as 3.45 GHz and the value of $L_{total} = sp_1$ (total length of resonating spiral 1) obtained is 24.28 mm. Here, sp_1 is the total length of spiral 1. By approximations, the design values of S and t_1 are taken as 1 mm. By substituting these values in Eqs. (5) and (6), the optimum value of L_{out} and N is calculated as 6 mm and 1.25 mm respectively. The length of spiral1 is optimized to 26.5 mm. Similarly for the WLAN band notch, for the resonance frequency of 5.4 GHz, the calculated $L_{total} = sp_2$ (the total length of resonating spiral 2) is 20 mm and the optimized values of L_{out1} and L_{out2} have been obtained as 6 and 4 mm respectively for the $t_1 = t_2 = S = 1$ mm. Where L_{out1} and L_{out2} are the outer turn side length of spiral 1 and spiral 2. The L_{out1} is equal to u_1 and L_{out2} is equal to u_2 for spiral and spiral 2 respectively. The third band notch for the Fixed/Mobile Satellite Communication (F/MSC) is achieved by introducing a half-wavelength spiral in the ground plane as shown in Figure 1. The resonance frequency of the spiral depends on the length (L_{out}) of the inductive arms and capacitive gap (S) of the spiral, as it is a self-resonating structure. Thus for optimum design and to achieve resonating frequencies the rectangular planner spirals are chosen as shown in Figure 1(c).

4. Results and discussions

To overcome the issue of interference in the UWB range, two planar spirals sp_1 (for WiMAX) and sp_2 (for WLAN) are capacitively coupled with the microstrip line for the band notch characteristic, and the third planar spiral is added in the ground plane. The parametric analysis is done for the optimum length of

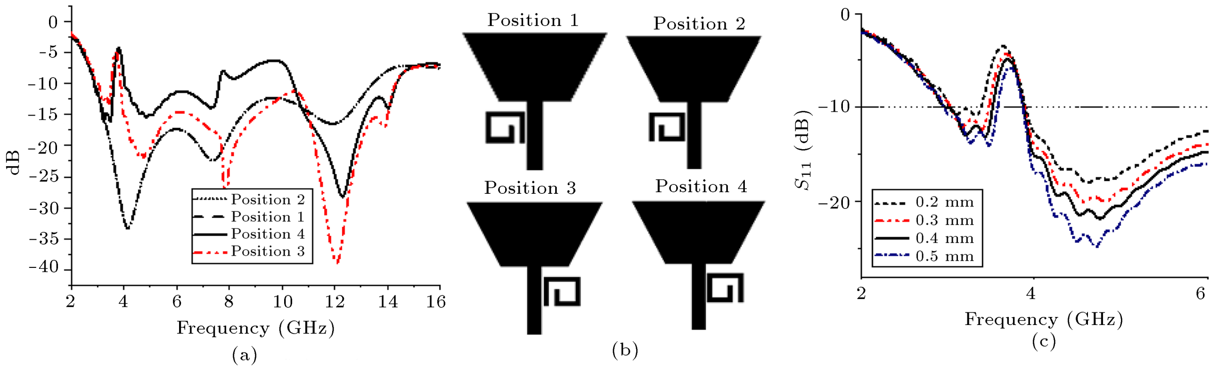

Figure 3. Simulated S_{11} for the parametric analysis of spiral 1 (a) variation of S_{11} for the position of spiral 1, (b) various positions of spiral1, and (c) variation of gap between feed and spiral 1.

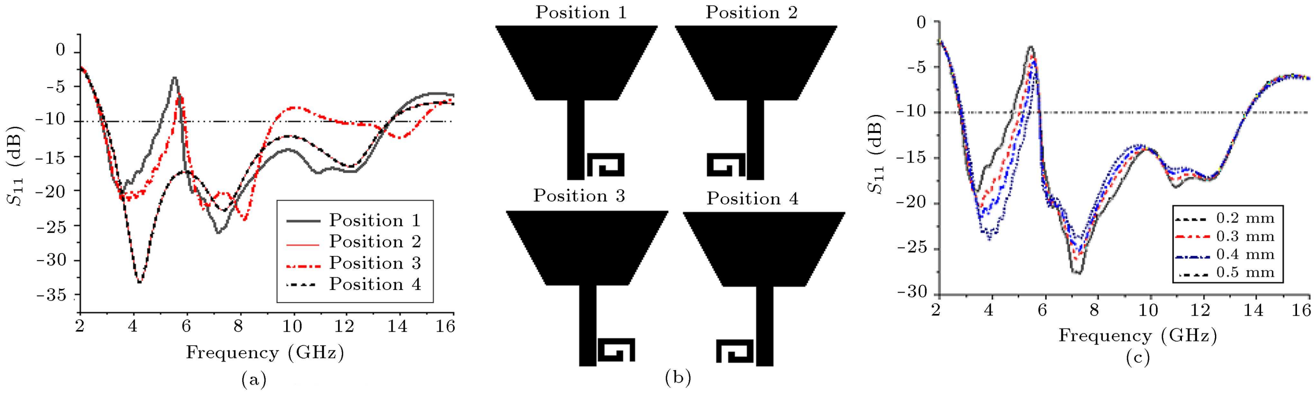

Figure 4. Simulated S_{11} for the parametric analysis of spiral 2 (a) variation of S_{11} for the position of spiral 2, (b) various positions of spiral 2, and (c) variation of gap between feed and spiral 2.

spirals, various positions of the spiral, and the spacing between the feed line and the spiral. The resultant characteristics are shown in Figure 3. Figure 3(a) and (b) show the positions of slot 1 and its S_{11} characteristics for various positions. Thus it can be observed that position 3 is the best among the positions considered. By keeping the slot in this position the effect of the gap between the feed line and spiral structure is observed as shown in Figure 3(c). It can be noted from Figure 3(c) that as the gap between the feed line and spiral increases by more than 0.4 mm the magnitude of the notch at the 3.5 GHz decreases and as the gap decreases by less than 0.4 mm the lower cut off frequency gets disturbed.

A similar parametric analysis is done for the WLAN spiral (sp_2) and the related results are displayed in Figure 4. From the obtained results, position 1 gives the optimum results. Also, the 0.3 mm gap between the feed line and a spiral is optimum for the WLAN characteristic. The third band notch for the F/MSC is achieved by introducing a half wavelength spiral in the ground plane. The optimization of the position and length (g1=gap between the ground and spiral 3 variations) of spiral 3 is shown in Figure 5. When the spiral resonator 3 is placed in position 3 and position 4, the notch at the desired frequency gets disappeared. From Figure 5(a) it can be observed that position1 gives the optimum result. When the gap between the ground and spiral 3 is 0.3 mm maximum bandwidth is obtained and the sharp band notch is achieved for the F/MSC band as shown in Figure 5(c).

The optimized dimensional parameters for spiral 1 to acquire band notch for WiMAX u_1 (L_{out1})=6 mm, $S = 1 = t_1 = 1$ mm, and hence the sp_1 is 26.5 mm. For spiral 2 the optimized dimensional parameters are u_2 (L_{out2})=4 mm, $S = 1 = t_2 = 1$ mm, and hence the sp_2 is 20 mm which secures the band notch for WLAN. The optimized dimensional parameters for spiral 3 to acquire band notch for F/MSC is u_3 (L_{out3})=3.5 mm, $u_4 = 3.8$ mm, $S = 1 = t_1 = 1$ mm and hence the $L_{total} = sp_3$ (Total length of resonating spiral 3) is 14.9 mm. The proper position, orientation, and lengths of the spirals decide the characteristics of band notches. The final design consists of a half hexagonal monopole with three resonating spirals to acquire triple-notch characteristics which are shown in Figure 1.

When all the three self-resonating spirals are added in the design, one in the ground and two coupled with the feed line sharp notches are obtained for WiMAX, WLAN, and F/MSC band. The return loss of

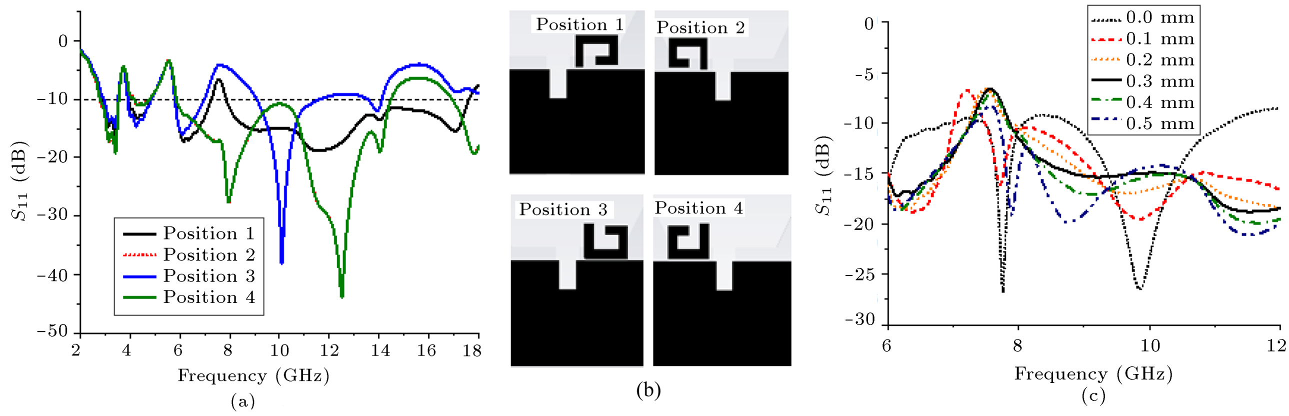

Figure 5. Simulated S_{11} for the parametric analysis of spiral 3, (a) variation of S_{11} for the various positions of spiral 3, (b) various positions of spiral 3, and (c) variation of gap between ground and spiral 3.

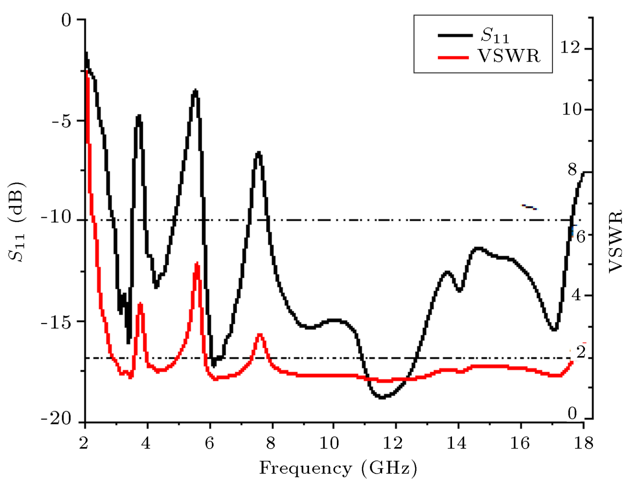

Figure 6. Simulated S_{11} and VSWR variation with frequency.

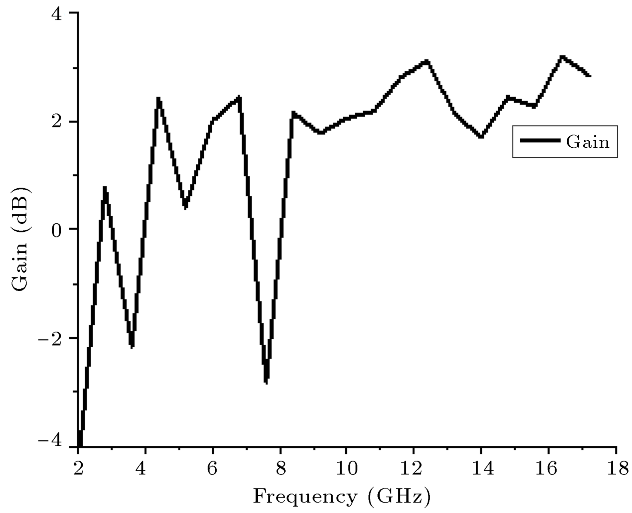

Figure 7. Simulated Gain variations with frequency.

less than –10 dB is obtained for the range 2.9 GHz–17.6 GHz excluding the three notches that are 3.4–3.8 GHz, 5.0–5.6 GHz, and 7.2–7.9 GHz as shown in Figure 6. The VSWR is also shown in Figure 6. The obtained gain for the proposed antenna is shown in Figure 7. From the graph, we can depict that a maximum gain of 3.1 dBi at 12.4 GHz is obtained, with a reduced gain of –2.08 dBi, 0.40 dBi and –2.6 dBi for band notch frequencies at 3.56 GHz, 5.5 GHz, and 7.62 GHz respectively.

To validate the antenna design the prototype is fabricated and the measured results are presented. The return loss measurements are carried out by using available VNA (Vector Network Analyzer, Model-MS2028C) and the radiation pattern is measured in the anechoic chamber. Figure 8 shows the fabricated antenna prototype and the concerning results are presented in Figures 9 and 10. It can be seen from Figure 8 that the simulated bandwidth ranges from 2.9–17.6 GHz and the measured bandwidth is in the range 3.21–18.0 GHz. The measured results

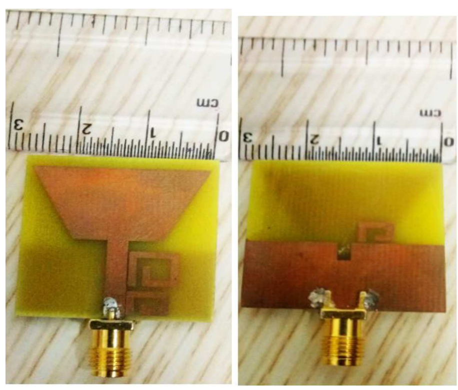

Figure 8. Front view and back view of fabricated prototype.

are slightly different from the simulated one, due to manufacturing tolerance and soldering. The production error (manufacturing) error is the main likely cause of the difference between simulated and measured results. During the fabrication, this error may occur

Table 2. Comparison of reported band notch antennas with proposed work.

Reference	Size (mm^2)	No. of notches	Substrate used	Bandwidth (GHz)
[2]	18×20	5 GHz (WLAN)	FR4	$3.12 - 10.73$
[3]	22×26	$3.8 - 4.28$ GHz (Wi MAX) 5.76-6.16 (WLAN)	RT 5880	$2.9 - 12$
[4]	10×13	5 GHz (WLAN)	FR4	$4.36 - 13.35$
[5]	28×52 22×24	$5.15 - 6.17$ (WLAN) $3.35 - 3.8$ GHz	FR4 FR4	$3.11 - 13.15$ $3.2 - 10.9$
[6]	22×24	$3.35 - 3.8$ GHz $5.12 - 5.84$ GHz	FR4	$3.2 - 10.9$
[7]	38.5×46.4	$5.0 - 5.5$ GHz $7.2 - 7.6$ GHz	Metamaterial based	$2 - 12.5$
[8]	39×35	5.5 GHz	RT/Duroid 4003	$3.1 - 10.6$
[9]	24×17	2.4 GHz Bluetooth $3.3 - 3.6$ GHz WiMAX $5.13 - 5.85$ GHz WLAN	RT Duroid 5880	
[10]	32×30	3.5 GHz 5.5 GHz	FR4	$2.8 - 12$ GHz
[11]	26×36.6	$5.15 - 5.85$ GHz	FR4	$2.9 - 20$ GHz
[13]	20×36	No. notch	FR4	$2.27 - 7.53$ GHz
[16]	32×24	5.2 GHz 8.2 GHz	Rogers RO3003	$3.1 - 13$
Proposed antenna	$\mathbf{28 \times 29}$	**3.6 GHz** **5.5 GHz** **7.54 GHz**	**FR4**	$\mathbf{3.2 - 18.00}$ **GHz**

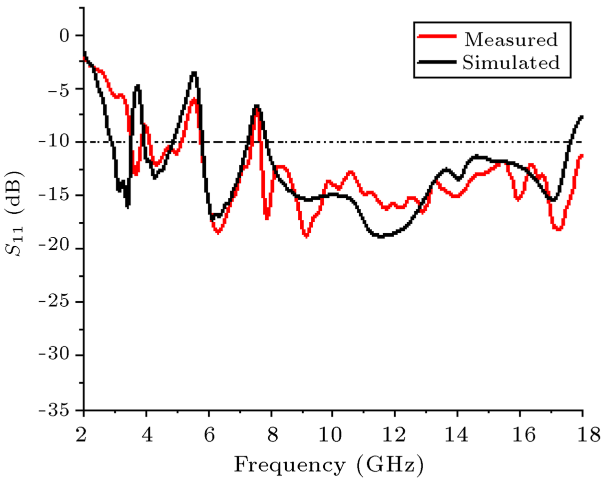

Figure 9. Simulated and measured return loss.

due to incorrect thickness of the substrate layer and dimension inaccuracies. Similarly, the measured and simulated radiation patterns at resonating frequencies are presented in Figure 10. The E-field is unidirectional at 3.1 GHz and 4.3 GHz. On the other hand, a bidirectional E- field is obtained at 6.3 GHz. The H-filed radiation pattern is bidirectional at all the resonating frequencies.

The surface current distribution is shown in Figure 11. The current is mainly concentrated in spiral 1 and edges of the patch at a lower resonating frequency. However, at higher resonating frequency i.e., at 4.3 GHz the current is flowing in spiral 1, spiral 2, and the antenna patch. At 6.2 GHz the current is mainly distributed in spiral 2 and spiral 3. The total efficiency and radiation efficiency of an antenna are presented in Figure 12. The efficiency s above 60% in the obtained impedance bandwidth and has been reduced below 40% at notch frequencies. The comparison of the proposed work with the reported work is shown in Table 2.

5. Conclusion

The stepwise realization of compact planner UWB antenna with triple notch characteristics is presented. The triple-notch characteristic is validated through simulated results. The impedance bandwidth for $VSWR < 2$ is obtained for the ultra-wide band in

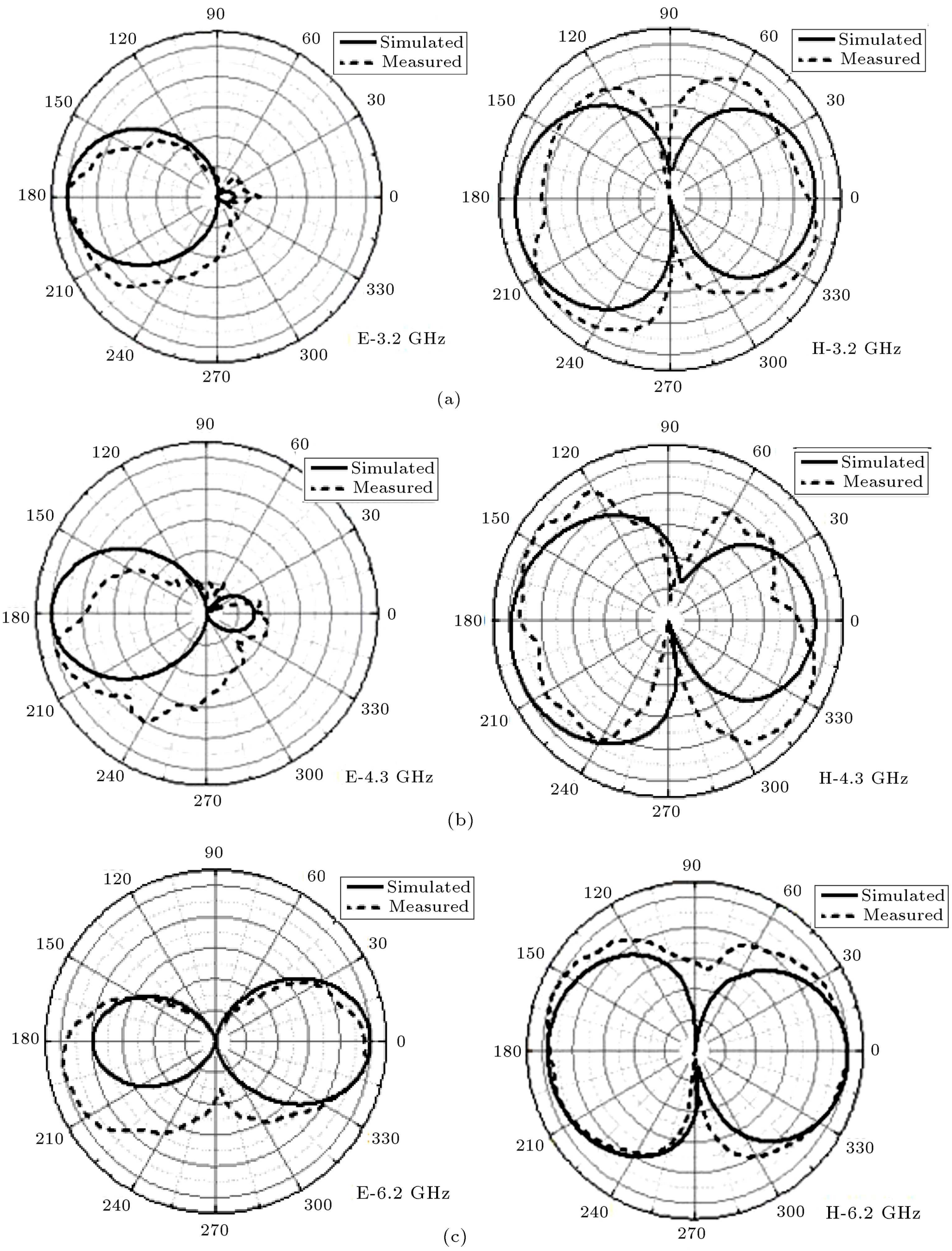

Figure 10. Radiation pattern at resonating frequenceies (a) 3.2 GHz; (b) 4.3 GHz; and (c) 6.2 GHz.

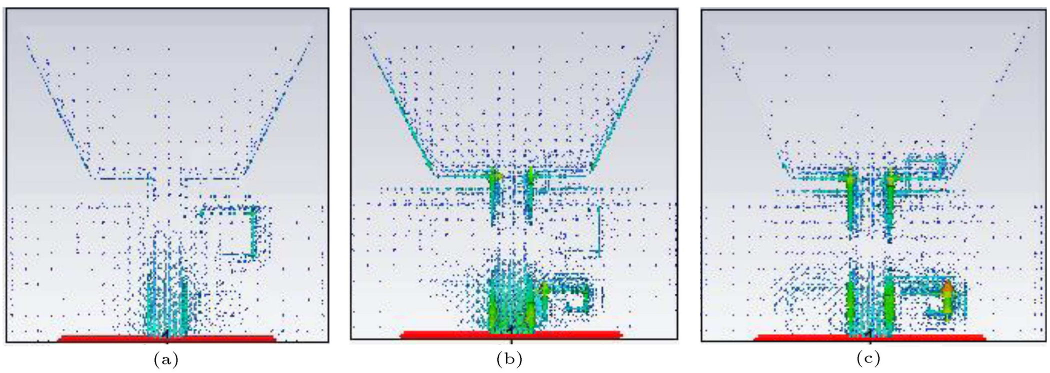

Figure 11. Surface current distributions for resonating frequenceies (a) 3.2 GHz; (b) 4.3 GHz; and (c) 6.2 GHz,

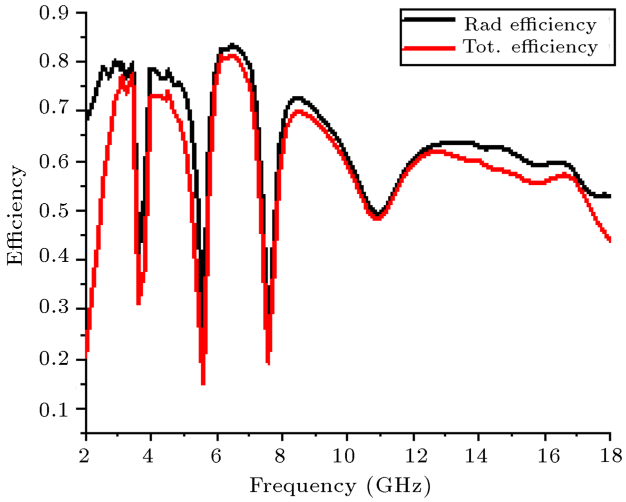

Figure 12. Variation of total efficiency and radiation efficiency,

the range of 3.2 GHz –18.00 GHz with triple band-notch for WiMAX, WLAN, and F/MSC band. The simulated gain is stable for passband frequency in the range of 0.9–3.21 dBi and gain is reduced to –2.08 dBi, 0.40 dBi, and –2.6 dBi at 3.57 GHz, 5.3 GHz, and 7.6 GHz respectively for notch bands.

References

1. FCC, Federal Communication Commission revision of part 15 of commission's rules regarding ultra-Wideband transmission systems", *First Report and Order FCC*, Washington, DC, **48** (2002).
2. Hong, S.H., Shin, J.W. Park, H., et al. "Analysis of band-stop techniques for UWB antennas", *Microw. Opt. Technol. Lett.*, **49**, pp. 1058–1062 (2007).
3. Jiang, D., Xu, Y., Xu, R., et al. "Compact dual-band-notched UWB planar monopole antenna with modified CSRR", *Electron. Lett.*, **48**(20), pp. 1250–1252 (2012).
4. Keshwala, U., Rawat, S., and Ray, K. "Compact circular monopole antenna with band notch characteristics for UWB applications", *5th International Conference on Signal Processing and Integrated Networks*, Noida, India, pp. 312–315 (2018).
5. Mondal, T. and Das, S. "UWB printed hexagonal monopole antennas with WLAN band rejection", *IEEE Antenna Week (IAW)*, Kolkata, India, pp. 1–4, (2011). DOI: 10.1109/IndianAW.2011.6264945.
6. Azim, R., Islam, M.T., and Mobashsher, A.T. "Design of a dual band-notch UWB slot antenna by means of simple parasitic slits", In *IEEE Antennas and Wireless Propagation Letters*, **12**, pp. 1412–1415 (2013). DOI: 10.1109/LAWP.2013.2288370.
7. Li, W.T., Hei, Y.Q., Feng W., et al. "Planar antenna for 3G/Bluetooth/WiMAX and UWB applications with dual band-notched characteristics", In *IEEE Antennas and Wireless Propagation Letters*, **11**, pp. 61–64 (2012). DOI: 10.1109/LAWP.2012.2183671.
8. Yazdi, M. and N. Komjani, "Design of a band-notched UWB monopole antenna by means of an EBG structure", *IEEE Antennas and Wireless Propagation Letters*, **10**, pp. 170–173 (2011).
9. Reddy, G.S., Chittora, A., Kharche, S., et al. "Bluetooth/UWB planar diversity antenna with WiMAX and WLAN band-notch characteristics", *Progress In Electromagnetics Research B.*, **54**, pp. 303–320 (2013). DOI: 10.2528/PIERB13080404.
10. Suo, Y., Li, W., and Wang, H. "A dual-band notched ultra-wideband microstrip antenna", *IEEE International Symposium on Antennas and Propagation and USNC/URSI National Radio Science Meeting*, San Diego, CA, USA, pp. 1787–1788 (2017).
11. Sanyal, R., Sarkar, P.P., and Chowdhury, S.K. "Quasi-self-complementary ultra-wideband antenna with band rejection characteristics", *International Journal of Microwave and Wireless Technologies*, **10**(3), pp. 336–344 (2018).
12. Jaglan, N., Gupta, S.D., Kanaujia, B.K., et al. "Band notched UWB circular monopole antenna with inductance enhanced modified mushroom EBG structures", *Wireless Network*, **24**, pp. 383–393 (2018). https://doi.org/10.1007/s11276-016-1343-7
13. Tiwari, R.N., Singh, P., and Kanaujia, B.K. "Asymmetric U-shaped printed monopole antenna embedded with T-shaped strip for bluetooth, WLAN/WiMAX applications", *Wireless Network*, **26**, pp. 51–61 (2020). https://doi.org/10.1007/s11276-018-1781-5
14. Ullah, S., Ahmad, S., Khan, B.A., et al. "An hp-shape hexa-band antenna for multi-standard wireless communication systems", *Wireless Network*, **25**, pp. 1361–1369 (2019). https://doi.org/10.1007/s11276-018-1760-x
15. Kumar, G. and Ray, K.P. "Broadband microstrip antennas", *Boston, London: Artech House, CH.*, **9**, pp. 362–71 (2003).
16. Yadav, D., Abegaonkar, M.P., Koul, S.K., et al. "A compact dual band notched UWB circular monopole antenna with parasitic resonators", *AEU-International Journal of Electronics and Communications*, **84**, pp. 313–20 (2018).
17. Babbar, P. and Keshwala, U. "Design of dual band-notch square patch antenna for UWB applications", *2020 7th International Conference on Signal Processing and Integrated Networks (SPIN)*, Noida, India, pp. 710–713 (2020). DOI: 10.1109/SPIN48934.2020.9071364.
18. Keshwala, U., Ray, K., and Rawat, S. "Honeycomb shaped fractal antenna with dual notch characteristic for UWB applications", *Scientia Iranica*, **9**(6), pp. 3338–3346 (2021). DOI: 10.24200/sci.2021.56585.4799
19. Keshwala, U., Rawat, S., and Ray, K. "A Novel small-scale heart shape monopole antenna with DGS for UWB", *2019 International Conference on Computational Intelligence and Knowledge Economy (ICCIKE)*, Dubai, pp. 36–39 (2019). DOI: 10.1109/ICCIKE47802.2019.9004402.

Acknowledgement

The authors like to acknowledge and convey their heartfelt thanks to Centre of Applied Research for Electronics (CARE), Indian Institute of Technology (IIT), Delhi for extending support in providing essential measurement facilities to complete this research work.

Biographies

Ushaben Keshwala is presently working as Assistant Professor in Electronics and Communication Department, Amity University Uttar Pradesh, India. She graduated with Bachelor of Engineering (BE) in Electronics and Communication from GH Patel College of engineering and Technology, VV Nagar, Gujarat, India in 2007. She did her M.Tech degree in the Electronics and Communication from Amity University Uttar Pradesh, India in 2013. She is pursuing PhD degree in the research area of planar antennas for wireless and satellite communication systems in. She has published 5 research papers in international IEEE/Springer conferences. Her current research interest includes Nature Inspired, Reconfigurable antennas for Wireless Communication and Pseudo random number generation for communication systems.

Sanyog Rawat is presently associated with Electronics and Communication Engineering Department, Manipal University Jaipur. He has been into teaching and research for more than fifteen years. He graduated with Bachelor of Engineering (BE) in Electronics and Communication, Master of Technology (M.Tech) in Microwave Engineering and PhD in the field of Planar Antennas. He has been engaged actively in the research areas related to planar antennas for wireless and satellite communication systems. He has published more than 60 research papers in peer-reviewed International Journals, Book series and IEEE/Springer conferences. He has organized several workshops, seminars, national and international conferences. He has been empaneled in the editorial and reviewer board of various national and International Journals. He has also edited the books on proceedings of the International conference on Soft Computing Theories and Applications (SoCTA-2016, 2017), proceedings of International Conference on Smart Systems, Innovations and Computing (SSIC-2017) and International Conference on Engineering Vibrations, Communication and Information Processing (ICoEVCI,2018) for Springer publication. His current research interests include reconfigurable RF printed circuits, passive and active microwave integrated circuits.

Kanad Ray is a Professor and Head of Physics department at the Amity School of Applied Sciences Physics Amity University Rajasthan (AUR), Jaipur, India. He has obtained M.Sc and PhD degrees in Physics from Calcutta University and Jadavpur University, West Bengal, India. In an academic career spanning over 22 years, he has published and presented research papers in several national and international journals and conferences in India and abroad. Some of his papers have more than 5 Impact Factor. He has authored a book on the Electromagnetic Field Theory. Prof. Ray's current research areas of interest include cognition, communication, electromagnetic field theory, antenna and wave propagation, microwave, computational biology, and applied physics. Presently he is guiding 8 PhD scholars in various interdisciplinary fields. He has been serving as Editor of different Springer Book Series. Presently he is an Associated Editor of Journal of Integrative Neuroscience published by IOS Press, Netherlands. He has travelled more than a dozen countries on different academic missions. He has established a MOU between his University and University of Montreal, Canada for various joint research activities. He has also established collaboration with National Institute for Materials Science (NIMS), Japan for joint research activities and visits NIMS as a visiting Scientist. He organizes international conference series such as SoCTA, ICOEVCI as General Chair.